THE JOURNAL OF PHYSICAL CHEMISTRY C

Article

pubs.acs.org/JPCC

Replacing the Al_2O_3 Shell on Al Particles with an Oxidizing Salt, Aluminum Iodate Hexahydrate. Part II: Synthesis

Dylan K. Smith,[†] Daniel K. Unruh,[‡] and Michelle L. Pantoya*[,†]

[†]Department of Mechanical Engineering, and [‡]Department of Chemistry, Texas Tech University, Lubbock, Texas 79409, United States

ABSTRACT: The main reaction mechanism that replaces the Al_2O_3 passivation layer on Al nanoparticles with an energetic AlH salt is demonstrated. The reaction mechanism is pH dependent and utilizes electrostatic forces that occur between the Al_2O_3 passivation layer and free hydrogen atoms (H^+) in solution. When Al particles are added to highly acidic solutions, free H^+ polarize the Al−O bonds in Al_2O_3, resulting in the formation of H_2O and free Al^{3+} cations that are complexed by water molecules and exist as $[Al(H_2O)_6]^{3+}$ in aqueous solutions. The concentration of AlH is limited by the amount of $[Al(H_2O)_6]^{3+}$ that forms from the polarization reaction between free H^+ and the initial Al_2O_3 concentration. The proposed mechanism describes a stoichiometric reaction, but deviations from the stoichiometric reaction are expected with varying equivalence ratios (ER). The polarization mechanism is confirmed by measuring deviations in concentration of final AlH mixtures as a function of ER. A salt formation theory dependent on pH and pK_a is used to demonstrate how the final AlH concentrations can be estimated at ER values that are not stoichiometric.

AlH Synthesis from Alumina and Iodic Acid

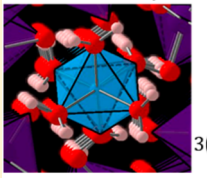

$$2Al_2O_3 + 12H_3O^+ + 12IO_3^- + 6HIO_3 \rightarrow$$
$$4Al^{3+} + 18H_2O + 12IO_3^- + 6HIO_3 \rightarrow$$
$$3[Al(H_2O)_6]^{3+} + Al^{3+} + 12IO_3^- + 6HIO_3 \rightarrow$$
$$3([Al(H_2O)_6]^{3+}(3IO_3^-)) + Al^{3+} + 3IO_3^- + 6HIO_3 \rightarrow$$
$$3([Al(H_2O)_6]^{3+}(3IO_3^-)(2HIO_3))_s + (\frac{1}{2}Al_2O_3)_s + (\frac{3}{2}I_2)_v + (\frac{3}{4}O_2)_v$$

INTRODUCTION

Aluminum nanoparticles inherently include a 3−5 nm thick aluminum oxide (Al_2O_3) passivation shell.[1] The Al_2O_3 shell acts as a barrier for oxygen diffusion reactions with the Al^0 core and also as a heat sink during combustion. Multiple studies have explored various passivation materials including fluoropolymers[2−5] to reduce the effect of the Al_2O_3 diffusion barrier. Jouet et al.[4] replaced the Al_2O_3 shell with perfluorotetradecanoic (PFTD) acid, and Kim et al.[3] extended this work to micron-scale Al particles using poly(tetrafluoroethylene) (PTFE). These polymers offer the potential of a highly reactive oxidizer, fluorine, in close proximity to the core enabling increased energy liberation upon Al reaction. Instead of a polymer, this study replaces the Al_2O_3 shell with an energetic salt: aluminum iodate hexahydrate (AlH), $[Al(H_2O)_6](IO_3)_3(HIO_3)_2$. Similar to the fluoropolymers, passivation by AlH provides the close proximity of two oxidizers, iodine and oxygen, to Al that is not oxidized (Al^0) in the Al nanoparticle core. When the Al_2O_3 shell is replaced with AlH, the preliminary results indicate startlingly high increases in reactivity with measured flame speeds as high as 3200 m/s.[6,7] The mechanism of AlH synthesis and the parameters affecting reactivity in AlH−Al^0 composite particle systems are not well understood and are the primary focus of this two-part article: AlH reactivity (Part I)[7] and AlH synthesis (Part II).

Chemical reactions between the aluminum oxide (Al_2O_3) passivation layer on Al nanoparticles and acidic electrolytes have been studied for the anodization processes.[8−12] In the anodization process, a voltage is applied across Al thin films to measure pore formation as a function of the voltage and pH of the electrolyte.[8] A similar mechanism is discussed in Smith et al.[6] for the formation of aluminum iodate hexahydrate (AlH). However, the mechanism of formation of Al^{3+} during the AlH synthesis process is not well understood but of importance for the design of Al-based energetic materials with heightened reactivity.

There are two primary mechanisms for the formation of Al^{3+} in acidic solutions.[8,10] The first mechanism is field-assisted dissolution where the electromagnetic forces from applied voltages and ions in solution oxidize Al^0 to Al^{3+} and pull Al^{3+} across the Al_2O_3 passivation layer. This process is described by the following chemical reaction.

$$Al(s) \rightarrow Al^{3+}(aq) + 3e^- \quad (1)$$

The mechanism is demonstrated in Wu et al.[8] The second mechanism for the formation of Al^{3+} in acidic solutions is shown in reaction 2.[12]

$$Al_2O_3(s) + 6H^+(aq) \rightarrow 2Al^{3+}(aq) + 3H_2O \quad (2)$$

Reaction 2 has been reported to have a minor role in the anodization process where an applied voltage is used to induce pore formation;[8] however, reaction 2 may have a greater effect in situations where there is no applied potential across the Al and solution. The resulting formation of $[Al(H_2O)_6]^{3+}$ is also a key component in the formation of AlH and is discussed below.

Aluminum iodate hexahydrate (AlH) is a reactive salt, and the formation of AlH can be explained using mathematical

Received: June 14, 2017
Revised: August 6, 2017

DOI: 10.1021/acs.jpcc.7b05805
J. Phys. Chem. C XXXX, XXX, XXX−XXX

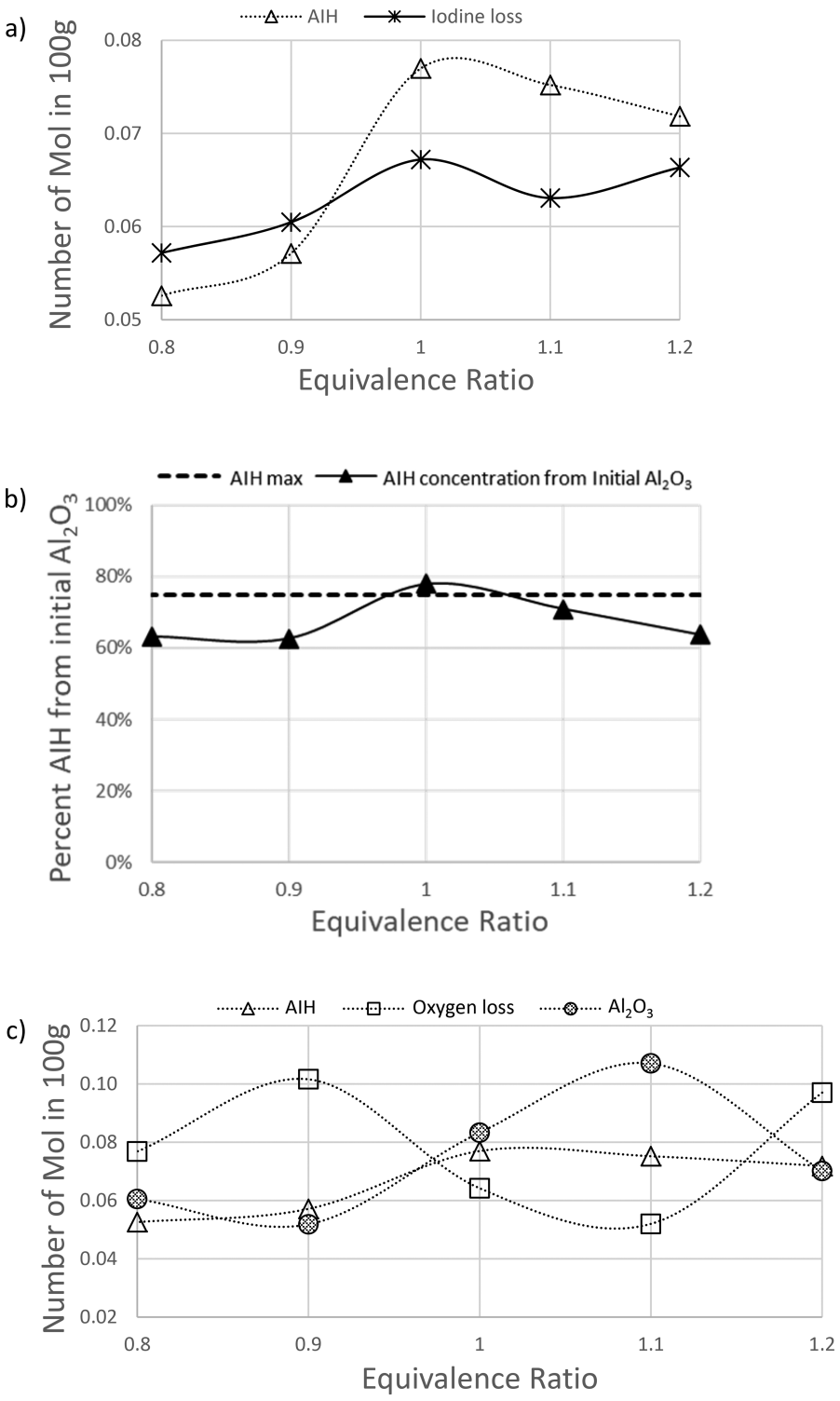

Figure 1. Graphics representing conditions obtained from reaction 3 (normalized to AIH concentration). (a) Iodine loss (*) and AIH concentration (Δ) in final AIH mixtures representing condition 1. (b) Solid line is AIH concentration divided by initial Al_2O_3 (▲), and the dashed line is the maximum AIH concentration (condition 2). (c) Oxygen loss (□), AIH (Δ), and Al_2O_3 (○ shaded) representing conditions 3 and 4.

descriptions of salt formation. Salt formation is a common and effective method for increasing solubility and dissolution rates of acidic and basic drugs.[13] The mathematical descriptions of salt formation from drug delivery research can be applied to describe the formation of AIH. Serajuddin et al.[14] showed that the formation of salts are related to the concentration, pH, and pK_a of the salt and acid (or base). The equations used to calculate solubility are shown in eqs 3a and 3b, where S is solubility of the acid or salt, $[A^-]$ is concentration of acid, [AH] is concentration of acid or salt, and pK_a and pH are the pH of solution and pK_a of either the salt or acid (subscript s means saturated solution).

$$S_{salt} = [AH]_s(1 + 10^{pK_a - pH}) \quad (3a)$$

DOI: 10.1021/acs.jpcc.7b05805
J. Phys. Chem. C XXXX, XXX, XXX−XXX

$$S_{acid} = [A^-]_s(1 + 10^{pH-pK_a}) \quad (3b)$$

Derivations of eqs 3a and 3b are shown in Serajuddin et al.,[14] along with detailed information on this mathematical formulation. In short, the formations of salts are determined by the max pH where the solubility of the salt and acid are equal. At pH max, both free acid and salt coexist as solids. If the pH of a saturated solution is lowered below pH max, salt will form. The solubility as a function of pH plots from Serajuddin et al.[14] are used to mathematically describe the formation of AIH.

It is important to note that Smith et al. (Part I)[7] focused on the reactivity of AIH mixtures and showed how the concentration of AIH, iodic acid, and material density affected the reactivity as measured by flame speed. Part II will focus on the synthesis conditions that affect the concentrations of AIH, Al^0, and iodic acids in AIH final mixtures. This will be accomplished by using concentration data from X-ray diffraction (XRD) analysis to predict species evolution that corresponds or deviates from established AIH reaction mechanisms and salt formation theory. The goal is to understand the synthesis method of AIH particles and determine the mechanism for how AIH increases reactivity in Al-based energetic materials. A better understanding of AIH could lead to enhance reaction rates for Al-based energetic materials, possibly approaching that of molecular explosives.

EXPERIMENTAL AND THEORETICAL DEVELOPMENT

The samples discussed in this article are the same samples used in Smith et al.,[7] and all details regarding mixing and testing are identical. For brevity, the reader is referred to Smith et al.[7] for an in-depth explanation of the mixing and testing procedures.

In Smith et al.,[6] a brief description on the formation of AIH was presented starting with the formation of Al^{3+} by electrostatic forces followed by hydrolysis of Al^{3+} to form aluminum hexahydrate $[Al(H_2O)_6]^{3+}$. Smith et al.[7] suggests that AIH replaces the Al_2O_3 passivation layer, and thus, a new mechanism for the formation of AIH from Al_2O_3 is proposed, following a similar mechanism presented by O'Sullivan.[12] When Al_2O_3 comes into contact with highly acidic solutions, polarization of Al_2O_3 molecules results in the formation of Al^{3+} and water following reaction 4.[12] Also, reaction 4 shows the polarization mechanism in reaction 2, with H_3O^+ instead of H^+, to form AIH.

$$2Al_2O_3 + 12H_3O^+ + 12IO_3^- + 6HIO_3 \rightarrow \quad (4a)$$

$$4Al^{3+} + 18H_2O + 12IO_3^- + 6HIO_3 \rightarrow \quad (4b)$$

$$3[Al(H_2O)_6]^{3+} + Al^{3+} + 12IO_3^- + 6HIO_3 \rightarrow \quad (4c)$$

$$3([Al(H_2O)_6]^{3+}(3IO_3^-)) + Al^{3+} + 3IO_3^- + 6HIO_3 \rightarrow \quad (4d)$$

$$3([Al(H_2O)_6]^{3+}(3IO_3^-)(2HIO_3))_s + \left(\frac{1}{2}Al_2O_3\right)_s + \left(\frac{3}{2}I_2\right)_v + \left(\frac{3}{4}O_2\right)_v \quad (4e)$$

Reaction 4a (initial reactants) and 4e (final products) represent the general global reaction for the formation of AIH from Al_2O_3 and reactions 4b, 4c, and 4d are the major intermediate steps needed to show the formation process of AIH from Al_2O_3. Each step in reaction 4 is shown as a forward reaction; however, it is suspected that many of the steps in reaction 4 are reversible and will reach an equilibrium state. The variables related to equilibrium conditions for reaction 4 are unknown; however, reaction 4 enables a comparison to measured concentration data (from XRD analysis) using specific details (conditions) that can be quantified as a function of equivalence ratio (ER) to validate reaction 4. Specifically, there are four conditions from reaction 4 as follows:

1. There is a 1:1 ratio of AIH concentration and iodine loss as shown in reaction 4e.
2. There is a maximum of 75% AIH concentration produced from initial Al_2O_3 shown by comparing initial concentration of Al_2O_3 (4a) and final concentration of Al_2O_3 (4e).
3. There is a 2:1 ratio of AIH concentration and oxygen loss as shown in reaction 4e.
4. There is a 6:1 ratio of AIH concentration to Al_2O_3 as shown in reaction 4e.

RESULTS AND DISCUSSION

The conditions from reaction 4 can be compared to concentrations of AIH mixtures as a function of equivalence ratio (ER) presented in Smith et al.,[7] and the maximum calculated uncertainty for the XRD measurements is 7.5%. Therefore, the error bars in the following results (i.e., Figures 1–6) are not included but are noted to all have a maximum uncertainty of 7.5%. The graphs representing variations in AIH and Al_2O_3 concentration and iodine and oxygen loss are shown in Figure 1a–c as a function of ER. All graphs in Figure 1 are normalized to AIH concentrations to represent conditions 1–4. Because all graphs in Figure 1 are normalized to AIH concentration, the lines representing iodine loss (Figure 1a), oxygen loss (Figure 1c), and Al_2O_3 concentration (Figure 1c) will be the same as AIH concentration in an ideal situation.

Reaction 4 assumes a stoichiometric concentration of IO_3^- and Al_2O_3 to form from AIH, and deviations are expected when the ER varies from stoichiometric as shown in Table 1.

Table 1. Deviations between XRD Measurements Shown in Figure 1 and Expected Values from Reaction 3 Normalized to AIH Concentration[a]

condition	min	max	ave
iodine loss	6%	16%	10%
AIH concentration	3%	12%	9%
oxygen loss	17%	78%	41%
Al_2O_3 concentration	2%	42%	15%

[a]Numbers in parentheses denote four conditions highlighted above.

In Table 1, the concentration of AIH has the smallest average deviation (9%), supporting the mechanism for formation of AIH shown in reaction 4. Three of the four average deviations in Table 1 are within 15% of the expected value from reaction 4 showing that, in general, the synthesis method that creates AIH follows the mechanism in reaction 4. The deviations from reaction 4 are caused by ancillary reactions that are occurring in solution as a result of difference in stoichiometry. Oxygen loss has the highest deviation because oxygen is in every molecule in solution, and most of the possible ancillary reactions will involve a transfer of oxygen. Iodine loss has the smallest deviation because it is involved in the least possible reactions.

DOI: 10.1021/acs.jpcc.7b05805
J. Phys. Chem. C XXXX, XXX, XXX–XXX

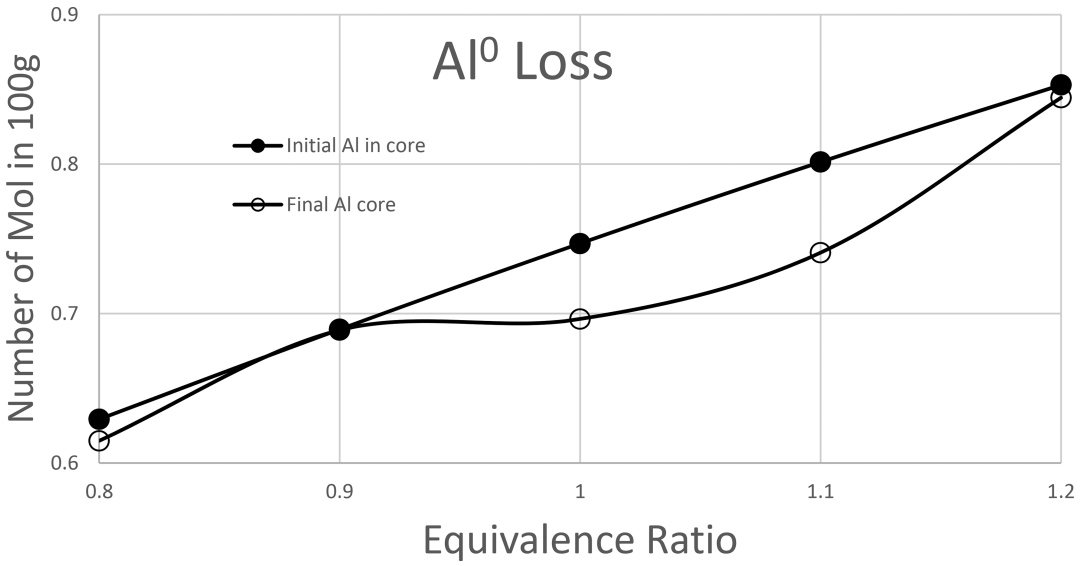

Figure 2. Concentration of Al_{core} (i.e., Al^0) initial (●) and Al_{core} final (○) as a function of equivalence ratio. Concentrations determined from XRD analysis.

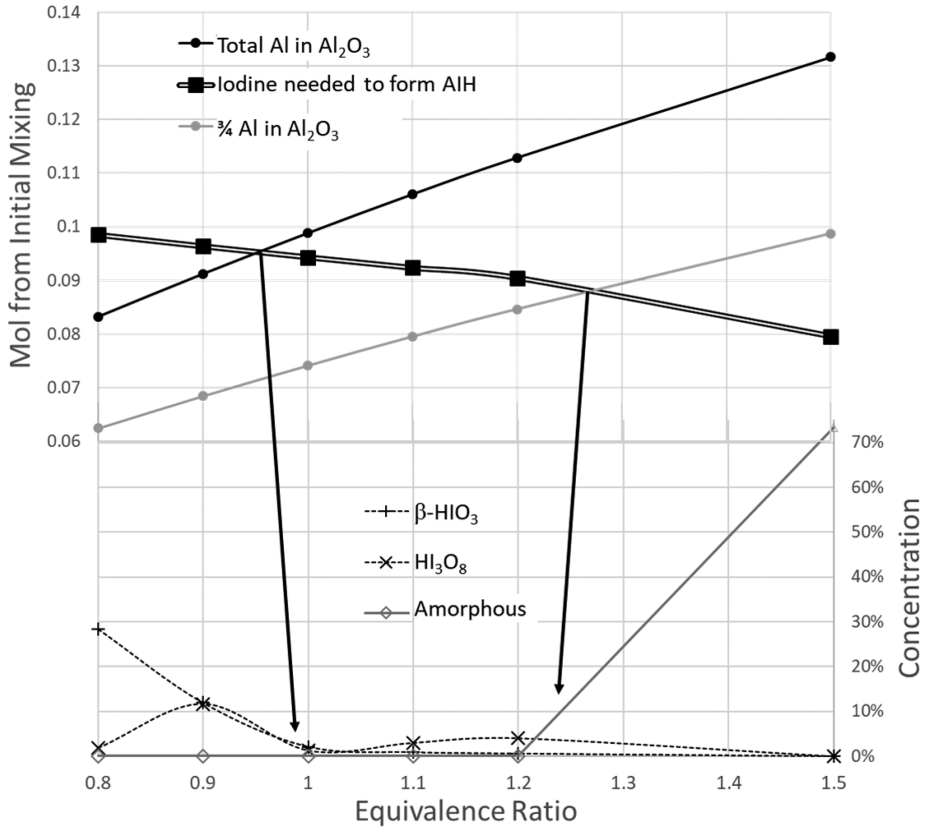

Figure 3. (Top) Solid black line is the number of moles of Al in Al_2O_3, gray line is 3/4 of the total number of moles of Al in Al_2O_3, and the double black line (solid □ markers) line is the iodine needed to form AIH (total iodine divided by 5) from initial mixing. (Bottom) Concentrations of β-HIO_3, HI_3O_8, and amorphous structure in final AIH mixtures from XRD measurements.

One example of an ancillary reaction is seen in Al^0 (Al_{core}) loss. The difference between $Al^0_{initial}$ and Al^0_{final} is shown in Figure 2. Above an ER of 0.9, a significant portion of Al^0 from the core is being oxidized (e.g., seen in Figure 2 as the difference between the two data points at ER 1.0). The most probable source of oxygen for the oxidation of Al^0 is from iodic acid or water shown in reactions 5a and 5b.

$$2Al + 3H_2O \rightarrow Al_2O_3 + 3H_2 \quad (5a)$$

$$2Al + HIO_3 \rightarrow Al_2O_3 + \frac{1}{2}H_2 + \frac{1}{2}I_2 \quad (5b)$$

Figure 1a shows that iodine loss is less than expected from reaction 4 above an ER of 0.9. Since iodine loss is less than expected and Al_{core} oxidation is greatest at ER = 0.9, Al_{core}

DOI: 10.1021/acs.jpcc.7b05805
J. Phys. Chem. C XXXX, XXX, XXX−XXX

oxidation is most likely from water and follows reaction 5a. The ancillary reactions that have an effect on the deviations shown in Table 1 are complicated by pH of the solution.

In every graph in Figure 1, a significant change in the trends can be seen between ER of 0.9 and 1.0 that is a result of pH. Figure 3 shows the relation between iodine needed to form AlH and Al from Al_2O_3 in initial mixtures. Since the iodine in AlH solutions comes from iodic acid, Figure 3 indirectly shows a relation to pH. Figure 3 shows the relation between Al in Al_2O_3 and iodine needed to form AlH in initial mixtures (top) and concentration data for β-HIO_3, HI_3O_8, and amorphous structure in final AlH mixtures (bottom). The solid black line in Figure 3 (top) is the total Al in initial mixtures including Al from Al_2O_3, and the gray line is 3/4 of Al in Al_2O_3 from initial mixtures. Both of these lines provide a reference for the Al that can be consumed from the Al_2O_3 shell according to reaction 3. In Figure 3, the double solid lines (solid □ markers) indicate the moles of iodine needed to form AlH from total iodine in initial mixing. The chemical formula for AlH is $[Al(H_2O)_6](IO_3)_3(HIO_3)_2$ such that there are five iodine molecules for every Al molecule. The double solid line in Figure 3 is the total moles of iodine in 100 g of initial mixtures calculated from initial mixing concentrations divided by 5 (i.e., to normalize the concentration data to fit the Al lines and represents the amount of iodine needed to form AlH from the available Al in Al_2O_3 in the initial mixtures). The bottom section of Figure 3 shows the concentrations of β-HIO_3, HI_3O_8, and amorphous material taken directly from the PXRD data in Smith et al.[7]

In Figure 3, we see that the line representing the amount of iodine needed to form AlH crosses (goes above) the full Al_2O_3 line (solid black line) between an ER of 0.9 and 1.0. When the iodine line crosses the full Al_2O_3 line, there is more iodine than is stoichiometrically needed to create AlH from the available Al in Al_2O_3. When compared to the concentration data for β-HIO_3 and HI_3O_8, the iodine line crosses the full Al_2O_3 line at the same ER where concentrations of β-HIO_3 and HI_3O_8 start increasing rapidly. The increase in β-HIO_3 and HI_3O_8 is expected when the iodine line crosses the full Al_2O_3 line because at this point, there is more IO_3^- in solution than needed to form AlH. Conversely, when the iodine line crosses (goes below) the 3/4 Al_2O_3 line between an ER of 1.2 and 1.5, the concentration of amorphous materials starts to increase (◇ line in Figure 3 bottom). If we assume only 3/4 of Al from Al_2O_3 forms AlH (from reaction 4), the iodine crossing the 3/4 Al_2O_3 line at the same point the amorphous structure begins shows that when there is not enough iodine to form AlH, an amorphous structure forms. Since the formation of β-HIO_3 and HI_3O_8 increases rapidly only after there is enough iodine to form AlH from all of the aluminum in the Al_2O_3 shell, all of the Al_2O_3 shell is reacting in the presence of the IO_3^- solution; however, amorphous formation starting after there is no longer enough iodine to form AlH from 3/4 of Al in Al_2O_3 shows that only a portion (3/4) of the original Al_2O_3 forms AlH. All of the Al_2O_3 is initially reacting with IO_3^- in solution, but only 3/4 forming AlH further supports the mechanism for the formation of AlH shown in reaction 4. Since the significant difference in trends in Figure 1 occurs at the same ER where there is more iodine needed to form AlH, Figure 3 also shows that the change in trends at an ER of 0.9 are a result of pH.

Reaction 4 assumes a stoichiometric mixture of Al_2O_3 and IO_3^-, and Figure 3 shows that the stoichiometric mixture for the formation of AlH occurs between an ER of 0.9 and 1.0. At an ER of 0.9, the Al_2O_3 and iodine loss have small deviations (Figure 1a and 1c) from the predicted mechanism. Figure 3 shows that when the ER is less than 0.9, there is more IO_3^- and H^+ in solution than needed for reaction 4. Specifically, for a stoichiometric mixture, there are five HIO_3 for every Al atom in Al_2O_3, and the $3H^+$ from the HIO_3 go toward the formation of water from oxygen in Al_2O_3. In acidic solutions, pH is defined as the negative log of the hydronium ion concentration, and pK_a is the pH where half of the H^+ are dissociated from its conjugate base. In reaction 4, the formation of water from oxygen in Al_2O_3 takes the free hydrogen (Brønsted acid) to form water and leaves a Lewis acid (Al^{3+}). The Al^{3+} cation is then coordinated by six water molecules under aqueous conditions, resulting in electron density being shifted from Al^{3+} to the oxygen in H_2O. This electron distribution lowers the energy needed to dissociate O−H bonds in $[Al(H_2O)_6]^{3+}$ by the amount of energy needed to disassociate $3H^+$ from $3HIO_3$.[15,16] The energy density (energy required per disassociation of each free hydrogen per mole of water) in this reaction changes because there is no difference in total energy, but the energy is spread out over six water molecules in $[Al(H_2O)_6]^{3+}$ instead of the three waters in the reaction between $3HIO_3$ and $3H_2O$. Because of the difference in energy density in the reaction described above, an apparent shift in pH and pK_a is expected.[17] Therefore, a mathematical model to describe the formation of AlH must be dependent on concentration, pH, and pK_a. Additionally, deviations from the mechanism shown in reaction 4 can be explained by salt formation theory.

Salt Formation. Serajuddin et al. present a mathematical description of salt formation based on solubility and a maximum pH where salts can form. The solubility of a salt is calculated by using concentration, pK_a, and pH as described previously in eqs 3a and 3b and can also be used to explain deviations from predicted concentrations as a function of the equivalence ratio (Table 1). Concentration and pH can be calculated from initial mixing parameters, and the pK_a of HIO_3 is 0.75; however, the pK_a of HI_3O_8 cannot be measured because HI_3O_8 and HIO_3 both dissolve into H_3O^+ and IO_3^- when in solution. Solubilities for both HIO_3 and HI_3O_8 using eqs 3a and 3b are shown in Figure 4, and pK_a for HI_3O_8 is estimated using the common ion effect based on an apparent pK_a shift,

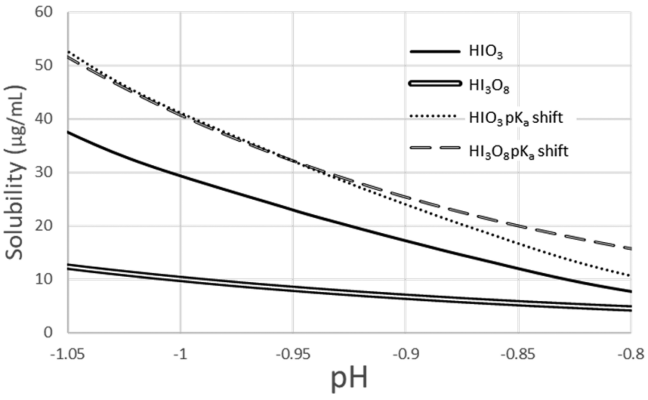

Figure 4. Solubility as a function of pH for HIO_3 and HI_3O_8 calculated from eq 2a. Solid black line indicates solubility of HIO_3 without pK_a shift, and the long-dashed line indicates solubility of HIO_3 with the pK_a shift. Double black line indicates solubility of HI_3O_8 without pK_a shift, and the short-dashed line indicates solubility of HI_3O_8 with the pK_a shift.

DOI: 10.1021/acs.jpcc.7b05805
J. Phys. Chem. C XXXX, XXX, XXX−XXX

Table 2. Low-Level IC Anion Analysis (ppm)

name	Fl	Cl	NO_2–N	Br	NO_3–N	PO_4	SO_4	hydration state
distilled new	<0.05	<0.05	<0.05	<0.05	<0.05	<0.05	<0.2	HIO_3
distilled aged	<0.05	0.06	<0.05	<0.05	<0.05	<0.05	<0.2	HIO_3
DI	<0.05	<0.05	<0.05	1.2	<0.05	<0.05	<0.2	HIO_3
HVAC chromAR	<0.05	<0.05	<0.05	<0.05	<0.05	<0.05	<0.2	HIO_3
not treated	<0.05	143.8	<0.05	<0.05	<0.05	<0.05	76.3	HI_3O_8

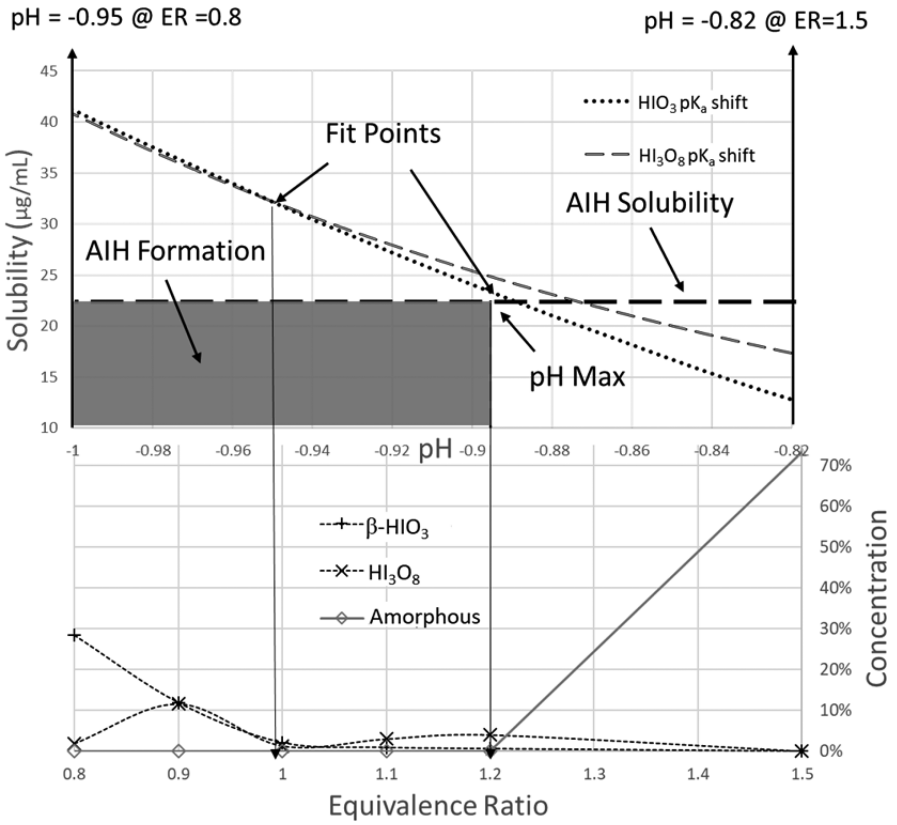

Figure 5. (Top) Solubility as a function of pH for HIO_3 and HI_3O_8 calculated from eq 2a with an apparent pK_a shift fit so HI_3O_8 solubility crosses HIO_3 solubility at an ER of 1.0. AIH solubility is estimated by fitting the AIH solubility line at pH max (AIH solubility and HIO_3 solubility are equal) to the point where an amorphous structure begins (ER 1.2 bottom). Shaded area labeled AIH formation represents the pH range where AIH will form. (Bottom) Concentration of β-HIO_3 (+), HI_3O_8 (×), and amorphous (◊) structure from XRD measurements.

discussed in Serajuddin et al.[14] By definition, the common ion effect is responsible for a change in solubility of an ionic precipitate when a soluble compound containing one of the ions in the precipitate is added to the solution in equilibrium with the precipitate.[14] This common ion effect is demonstrated in Table 2 when different "qualities" of water were mixed with I_2O_5 and then precipitated. Ion chromatography (IC) analysis was performed on the water samples, and PXRD quantitative analysis was performed on the precipitates. Table 2 supports the hypothesis that when Cl^- and SO_4^- ions are present in high concentrations, the IO_3^- solution precipitates out as HI_3O_8 instead of HIO_3. The relative humidity during precipitation was not measured; however, all samples were mixed within 10 min of each other and dried within a 10 cm radius of each other. Therefore, effect of relative humidity should be negligible between samples.

When any of the hydration states of iodine oxide (HIO_3, HI_3O_8, or I_2O_5) are mixed in water, a H^+-rich IO_3^- solution is formed. As water in solution evaporates, the H^+ in solution are more attracted to SO_4^- than IO_3^- because the pK_a of HSO_4^- (1.92) is greater than the pK_a of HIO_3. When the IO_3^- solution evaporates and a portion of the H^+ bonds with SO_4^- instead of IO_3^-, there is not enough H^+ to form HIO_3, resulting in HI_3O_8 (Table 2). The stable iodine oxides that form from IO_3^- solutions are HIO_3, HI_3O_8, and I_2O_5.[18] When there is not enough free hydrogen to form HIO_3, HI_3O_8 is formed. In this way, the common ion effect for HIO_3 can be thought of physically as an ion that takes free hydrogens that are needed to form HIO_3 from the IO_3^- solution. In short, Table 2 shows that HI_3O_8 will not precipitate from IO_3^- solutions unless there are less H^+ than needed to form HIO_3.

Figure 4 shows how the common ion effect can be used to estimate pK_a for HI_3O_8 with the solid lines representing the solubility of HIO_3 and HI_3O_8 assuming the same pK_a for both HIO_3 and HI_3O_8. The dashed lines in Figure 4 represent the solubility of HIO_3 and HI_3O_8 shifted by a change in apparent pK_a. Because the apparent pK_a shift will be less pronounced for compounds with higher solubilities,[14] the shift of pK_a as a function of pH for HI_3O_8 is twice that of HIO_3. Figure 4 also shows that when the apparent shift in pK_a is estimated in this way, the solubility of HI_3O_8 crosses the HIO_3 solubility line. The distance from the solubility line to 0 represents a

DOI: 10.1021/acs.jpcc.7b05805
J. Phys. Chem. C XXXX, XXX, XXX−XXX

probability of formation for each of the species (i.e., HIO_3 or HI_3O_8), and the greater the distance between the solubility line and 0, the greater the probability that HIO_3 or HI_3O_8 will form. By comparing the solubility lines with and without an apparent pK_a shift, Figure 4 shows that formation of HI_3O_8 is never favored over HIO_3 in low ion solutions, but when the ion effect is taken into account, HI_3O_8 becomes favored when the pH is above −0.95.

The mathematical model shown in Figure 4 provides an excellent way to quantify the common ion effect and explain what is occurring in Table 2. This method for estimating the pK_a of HI_3O_8 can be extended to AIH mixtures as a function of ER study by examining concentration as a function of solubility (Figures 5 and 6) and can help explain the deviations from the final AIH concentrations (Table 1) as predicted by reaction 4.

Figure 5 shows solubility as a function of pH for HIO_3 and HI_3O_8 in the calculated pH range for the ER study in the top plot and concentrations of β-HIO_3, HI_3O_8, and amorphous material as a function of ER (bottom plot). In Figure 5, the apparent pK_a shift is fixed so the HIO_3 solubility line crosses the HI_3O_8 solubility line at an ER of 1.0, the point where HIO_3 concentration increases and HI_3O_8 concentration starts to decrease. The maximum pH corresponding to AIH formation is labeled as max pH in Figure 5 and is where the solubility lines for AIH and HIO_3 intersect. Below the max pH, AIH will precipitate from solution. Because AIH will only form below the max pH, the AIH solubility line in Figure 5 is fit so pH max is below the pH (and equivalent ER) where an amorphous structure begins to form (ER of 1.1). When the apparent pK_a shift is fit to an ER of 1.0, and the solubility of AIH is fit to an ER of 1.2, Figure 5 can explain all of the iodic acid concentrations that were measured. Between an ER of 1.0 and 1.2, HI_3O_8 and HIO_3 concentrations are similar to the distance between the respective solubility lines and the solubility line of AIH. When the HIO_3 and HI_3O_8 solubility lines cross, the distance between the solubility lines and AIH line follows a similar trend as HIO_3 and HI_3O_8 concentrations (Figure 5 bottom, ER of 0.9 and 0.8).

Figure 5 shows how the solubility as a function of pH accounts for the iodic acid concentrations seen in the AIH mixtures but cannot solely account for AIH concentrations seen in AIH mixtures. Figure 6 (bottom) shows that AIH concentration decreases with ER from stoichiometric conditions and the difference between the HIO_3 line and AIH solubility line is greater than the concentrations seen in AIH mixtures. The discrepancies in AIH concentrations in Figure 6 are a result of using measured data to fit the apparent pK_a shift and AIH solubility. The pK_a for HI_3O_8 is estimated from a critical point where HIO_3 concentration increases and HI_3O_8 decreases (ER 0.9) and the solubility of AIH can be estimated because pH max was fit to the point where amorphous structure formation begins. Using this method to fit the apparent pK_a shift and AIH solubility gives average solubility between the two fitting points and not the solubility for each individual ER. The solubility calculations in Figure 6 are only estimates used to show how salt formation theory can be used to explain deviations from eq 3.

In Figure 3, we showed that at an ER of 0.9, there was more IO_3^- than needed to form AIH out of the Al_2O_3 shell. The common ion in AIH solubility plots would be $[Al(H_2O)_6]^{3+}$ and would behave in a similar manner to chlorine and sulfate anions in Table 2. The common ion effect in Figures 5 and 6 is caused by the reactions between H^+ with Al_2O_3 to form

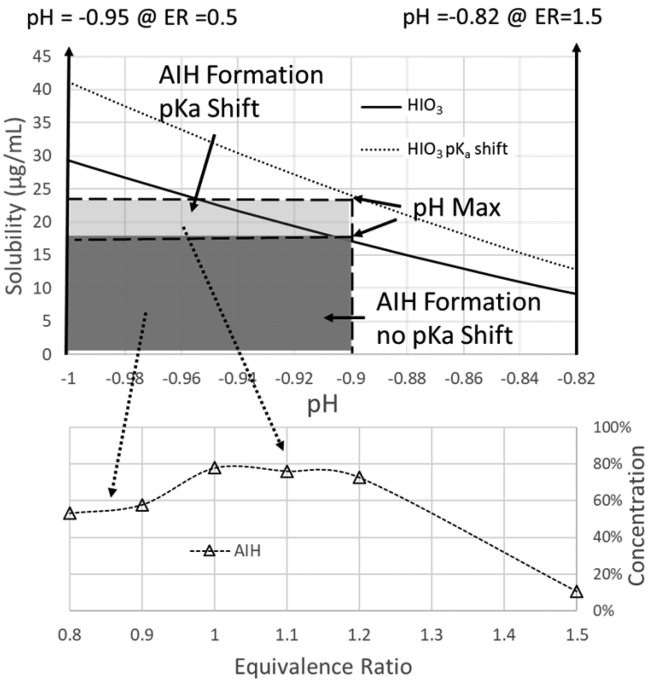

Figure 6. (Top) Solubility as a function of pH for HIO_3 calculated from eq 2a with and without an apparent pK_a shift. AIH solubility is estimated by fitting where the AIH solubility line intersects the HIO_3 solubility lines (with and without apparent pK_a shift) at ER 1.2. (Bottom) AIH concentration from XRD measurements.

$[Al(H_2O)_6]^{3+}$. When there are more IO_3^- anions than needed to form AIH from Al_2O_3, the result is more H^+ in solution, thereby reducing the common ion effect. This reduction in the common ion effect and its relation to AIH concentration are shown in Figure 6.

Figure 6 shows that the concentration of AIH is reduced when the solubility of HIO_3 is reduced. When there are more IO_3^- than the stoichiometric mixture in reaction 4, IO_3^- becomes less soluble. When IO_3^- is less soluble, pH max (intersection of AIH solubility and IO_3^- solubility) shifts, and the distance between the AIH solubility line and 0 is reduced. It is important to note that the solubility plots shown are estimates based on two fitting points at different ERs. For solubility plots based on measurements, the solubility lines will shift at every ER. In Figure 4, the HIO_3 and HI_3O_8 solubility lines without the pK_a shift represent an ER of 0, and the HIO_3 and HI_3O_8 solubility lines with a pK_a shift represent an average solubility between an ER of 1.0 and 1.2 (fitting points). Figure 4 shows the general trend that is expected of HIO_3 solubility resulting from the common ion effect in AIH synthesis using this mixing procedure. As ER and pH increase, HIO_3 solubility increases up to the stoichiometric mixture in reaction 3. The relation between HIO_3 solubility and ER is used in Figure 6 to estimate AIH concentrations. Using the trend in HIO_3 solubility from Figure 4 and adjusting the pH max in Figure 6 based on HIO_3 solubility only works if the solubility of AIH is directly related to that of HIO_3. Figure 2 in Li et al.[19] shows the assumption that pH max of salt with a conjugate free base (IO_3^-) is directly dependent on the solubility of the free base. The solubility trend in Figure 2 of Li et al.[19] closely follows the trend expected in AIH mixture using Figure 4 to estimate the common ion effect and Figure 6 to calculate concentration of AIH. Using the methods described in Figures 4−6, final

DOI: 10.1021/acs.jpcc.7b05805
J. Phys. Chem. C XXXX, XXX, XXX−XXX

concentrations of AIH mixtures can be estimated and used to optimize AIH mixtures for maximum reactivity.

CONCLUSIONS

The basic reaction mechanism that replaces the Al_2O_3 passivation layer with AIH reactive salt is presented in reaction 3. The reaction mechanism is pH dependent and utilizes electrostatic forces that occur between the Al_2O_3 passivation layer and H^+ in solution. When Al particles are added to highly acidic solutions, H^+ polarize the Al−O bonds in Al_2O_3. When the Al−O bonds are polarized, H_2O is formed from H^+ and oxygen in Al_2O_3, resulting in the formation of $[Al(H_2O)_6]^{3+}$. Concentration of AIH is limited by the amount of $[Al(H_2O)_6]^{3+}$ that forms from the polarization reaction between free hydrogens and initial Al_2O_3. The reaction mechanism describing the formation of AIH results in conditions that are used to support the validity of this mechanism. Iodine loss is expected to be the most accurate condition from the reaction mechanism, and the average deviation seen from PXRD measurements is 10%, supporting the polarization mechanism for the formation of AIH.

The polarization mechanism shown in reaction 4 assumes a stoichiometric mixture, and deviations from this mechanism are a result of varying ER. The final concentrations of AIH mixtures can also be estimated from salt formation theory by calculating the solubility as a function of pH and pK_a. The reaction mechanism includes a step that forms a Lewis acid from a Brønsted acid that will appear as a shift in pK_a. The shift in pK_a is used to demonstrate how salt formation theory can estimate final AIH concentrations. The basic reaction mechanism and salt formation theory can be used to tailor AIH concentrations to independently study the effects of AIH concentrations on reactivity. Independently studying the effects of concentration on AIH mixtures could result in increasing the reactive power with flame speeds higher than the 3200 m/s already measured.

AUTHOR INFORMATION

Corresponding Author

*Phone: 806-834-3733. E-mail: michelle.pantoya@ttu.edu.

ORCID

Michelle L. Pantoya: 0000-0003-0299-1832

Notes

The authors declare no competing financial interest.

ACKNOWLEDGMENTS

The authors are grateful for support from the Army Research Office under award W911NF-14-1-0250 and encouragement from our program manager, Dr. Ralph Anthenien. Dr. Andrew Jackson from TTU Civil Engineering Department is gratefully acknowledged for assistance with anion analysis of water samples.

REFERENCES

(1) Gesner, J.; Pantoya, M. L.; Levitas, V. I. Effect of Oxide Shell Growth on Nano-Aluminum Thermite Propagation Rates. *Combust. Flame* **2012**, *159* (11), 3448−3453.

(2) Skulski, L. Organic iodine(I, III, and V) Chemistry: 10 Years of Development at the Medical University of Warsaw, Poland. *Molecules* **2000**, *5* (12), 1331−1371.

(3) Kim, K. T.; Kim, D. W.; Kim, C. K.; Choi, Y. J. A Facile Synthesis and Efficient Thermal Oxidation of Polytetrafluoroethylene-Coated Aluminum Powders. *Mater. Lett.* **2016**, *167*, 262−265.

(4) Jouet, R. J.; Warren, A. D.; Rosenberg, D. M.; Bellitto, V. J.; Park, K.; Zachariah, M. R. Surface Passivation of Bare Aluminum Nanoparticles Using Perfluoroalkyl Carboxylic Acids. *Chem. Mater.* **2005**, *17* (11), 2987−2996.

(5) Jouet, R. J.; Carney, J. R.; Granholm, R. H.; Sandusky, H. W.; Warren, A. D. Preparation and Reactivity Analysis of Novel Perfluoroalkyl Coated Aluminium Nanocomposites. *Mater. Sci. Technol.* **2006**, *22* (4), 422−429.

(6) Smith, D. K.; Bello, M. N.; Unruh, D. K.; Pantoya, M. L. Synthesis and Reactive Characterization of Aluminum Iodate Hexahydrate Crystals $[Al(H_2O)_6](IO_3)_3(HIO_3)_2$. *Combust. Flame* **2017**, *179*, 154−156.

(7) Smith, D. K.; Unruh, D. K.; Wu, C.-C.; Pantoya, M. L. Replacing the Al_2O_3 Shell on Al Particles with an Oxidizing Salt, Aluminum Iodate Hexahydrate. Part I: Reactivity. *J. Phys. Chem. C* **2017**, DOI: 10.1021/acs.jpcc.7b05803.

(8) Wu, Z.; Richter, C.; Menon, L. A Study of Anodization Process During Pore Formation in Nanoporous Alumina Templates. *J. Electrochem. Soc.* **2007**, *154* (1), E8.

(9) Thompson, G.; Furneaux, R. C.; Wood, G. C.; Richardson, J. a.; Goode, J. S. Nucleation and Growth of Porous Anodic Films on Aluminium. *Nature* **1978**, *272*, 433−435.

(10) Diggle, J. W.; Downie, C. T.; Goulding, C. W. Anodic Oxide Films on Aluminum. *Chem. Rev.* **1969**, *69* (3), 365−405.

(11) Hoar, T. P.; Mott, N. F. Mechanism for the Formation of Porous Anodic Oxide Films on Aluminum. *J. Phys. Chem. Solids* **1959**, *9*, 97−99.

(12) O'Sullivan, J. P.; Wood, G. C. The Morphology and Mechanism of Formation of Porous Anodic Films on Aluminium. *Proc. R. Soc. London, Ser. A* **1970**, *317*, 511−543.

(13) Blagden, N.; de Matas, M.; Gavan, P. T.; York, P. Crystal Engineering of Active Pharmaceutical Ingredients to Improve Solubility and Dissolution Rates. *Adv. Drug Delivery Rev.* **2007**, *59* (7), 617−630.

(14) Serajuddin, A. T. M. Salt Formation to Improve Drug Solubility. *Adv. Drug Delivery Rev.* **2007**, *59* (7), 603−616.

(15) Akitt, J. W. Significance of Anion Effects in the Determination of Dissociation Constants of Strong Acids by Proton Nuclear Magnetic Resonance Spectroscopy. *J. Chem. Soc., Faraday Trans. 1* **1982**, *78*, 607−609.

(16) Akitt, J. W. Multinuclear Studies of Aluminum Compounds. *Prog. Nucl. Magn. Reson. Spectrosc.* **1989**, *21*, 1−149.

(17) Grunwald, E.; Fong, D. Acidity and Association of Aluminum Ion in Dilute Aqueous Acid. *J. Phys. Chem.* **1969**, *73* (3), 650−653.

(18) Selte, K.; Kjekshus, A.; Ekwall, P.; Smidsrod, O. Iodine Oxides Part II on the System H_2O I_2O_5. *Acta Chem. Scand.* **1968**, *22*, 3309−3320.

(19) Li, S.; Wong, S.; Sethia, S.; Almoazen, H.; Joshi, Y. M.; Serajuddin, A. T. M. Investigation of Solubility and Dissolution of a Free Base and Two Different Salt Forms as a Function of pH. *Pharm. Res.* **2005**, *22* (4), 628−635.

DOI: 10.1021/acs.jpcc.7b05805
J. Phys. Chem. C XXXX, XXX, XXX−XXX